Integrated CMOS Spectrometer for Multi-Dimensional NMR Spectroscopy

Dongwan Ha
Analog Devices, Inc.
Wilmington, USA
dongwan.ha@analog.com

Nan Sun
University of Texas at Austin, USA
nansun@mail.utexas.edu

Jeffrey Paulsen, Yiqiao Song, Yiqiao Tang, Sungjin Hong
Schlumberger-Doll Research
Cambridge, MA
jlpaulsen@slb.com, ysong@slb.com

Donhee Ham
Harvard University
Cambridge, MA
donhee@seas.harvard.edu

***Abstract*—This paper reviews our portable multi-dimensional nuclear magnetic resonance (NMR) spectroscopy system combining a 4-mm^2 CMOS NMR spectrometer integrated circuit (IC) and a permanent magnet. The work was first reported in [1] with emphases on overall system development and spectroscopy experimentations. Here we pay more attention to the IC design. The scalability of the integrated spectrometer can enable not only portable NMR spectroscopy in conjunction with small permanent magnets for in-field and online applications, but also parallel NMR spectroscopy for high-throughput applications.**

Keywords—NMR spectroscopy, portable NMR, CMOS integrated circuits, RF integrated circuits, biotechnology, biomolecular spectroscopy, biomolecular sensing.

I. Introduction

Nuclear magnetic resonance (NMR) spectroscopy is a powerful technique to examine molecular structures and dynamics with atomic resolution. It has served as a paramount tool in many branches of science and technology, with notable examples including organic chemistry, biochemistry, structural biology, metabolomics, and drug discovery [2]-[4]. An NMR spectroscopy instrument consists of a magnet to provide a static magnetic field and an NMR spectrometer electronics to manipulate and monitor the motions of nuclear spins via generation and detection of RF magnetic fields.

Traditional NMR spectroscopy instrumentation uses a large superconducting magnet, because its strong and highly homogenous field leads to the fine spectral resolution necessary for interrogating large molecules, such as proteins [5]. In fact, the study of such macromolecules is one frontier application of NMR spectroscopy. However, the fine spectral resolution of the bulky superconducting magnet may not be necessary for a range of small-molecule applications in chemistry, biotechnology, and chemical engineering. For these applications, small (thus portable) and low-cost permanent magnets with weaker fields would make NMR spectroscopy more broadly available, enabling in-field, on-demand, or online applications. This has been a strong motivation to develop permanent magnets with high enough field homogeniety for NMR spectroscopy [6].

Complementing this advance in magnet miniaturization, we integrated the NMR spectrometer electronics into a 4-mm^2 CMOS chip (Fig. 1). Furthermore, to show the overall system

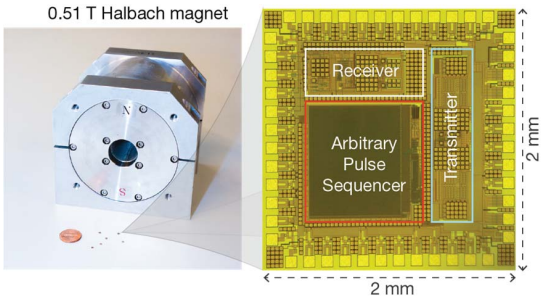

Figure 1. Our NMR spectroscopy system combining a 4-mm^2 NMR spectrometer IC and a 0.51-T NdFeB permanent magnet. This work was originally reported in Ref. [1].

miniaturization, we operated these chips with a compact 0.51-T permanent magnet (Fig. 1), conducting a variety of one-dimensional (1D) and two-dimensional (2D) NMR spectroscopy expeirments on various organic, biological, and drug compound molecules. We reported this advance in the *Proceedings of National Academy of Sciences* in 2014 [1]. The present paper is a review of this published work and borrows some materials from there, but at the same time the present paper focuses more on the design of the CMOS NMR spectrometer integrated circuit (IC). This complements the prior paper [1] focused more on the overall system and spectroscopy expreimentations.

We note that this work builds on, and is an advance from, prior ICs developed for NMR spectroscopy [7]-[9]. The prior works were limited to 1D spectroscopy [7]-[9], relied on external RF magnetic field pulse sequencers [9], and were experimented only with superconducting magnets [7]-[9]. By contrast, our IC has a higher degree of integration, allowing for arbitrary on-chip RF pulse sequence generation and thus multi-dimensional spectroscopy. Further, we used it with the small permanent magnet. In addition to the use for portable NMR spectroscopy, such scalable CMOS spectrometer chips may one day be useful for high-throughput analysis via parallelization.

978-1-5090-6389-5/17/$31.00 ©2017 IEEE

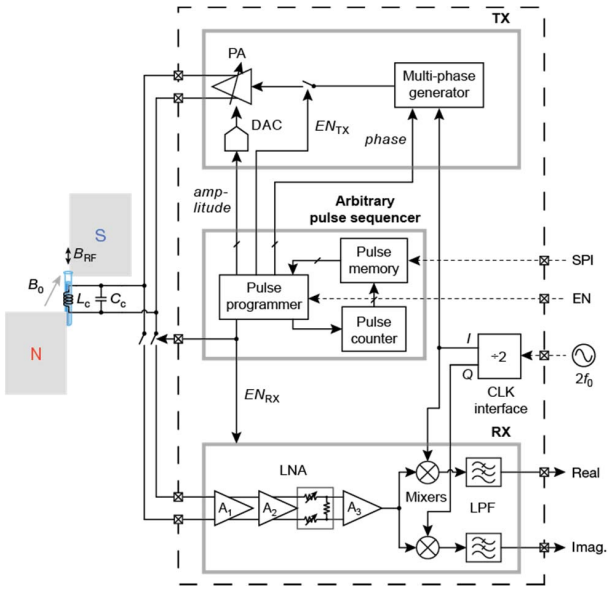

Figure 2. Architecture of the NMR spectrometer IC.

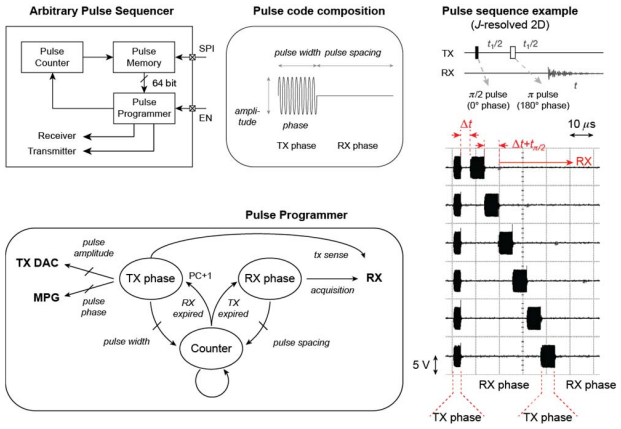

Figure 3. Arbitrary pulse sequencer.

II. Design of the NMR Spectrometer IC

Our NMR spectrometer IC consists of an RF transmitter (TX), an RF receiver (RX), and an arbitrary pulse sequencer (APS) (Fig. 2). The APS controls various parts of the TX to generate an RF pulse sequence with any desired durations, phases, and amplitudes of RF pulses and any desired intervals between RF pulses. Concretely, the APS controls the amplitude of each RF pulse via the DAC that sets the driving power of the power amplifier; the APS determines the phase of each RF pulse by controlling the multi-phase generator (MPG); and the APS sets the duration of each RF pulse and intervals between RF pulses by turning on and off the input signal path to the power amplifier. In this way, the TX can transmit desired RF pulse sequences into the NMR coil (L_c) so that the nuclear spin motions are manipulated in a broad variety of ways for various multi-dimensional spectroscopy experiments. The APS also controls the RX by, for example, turning it off when the TX is turned on.

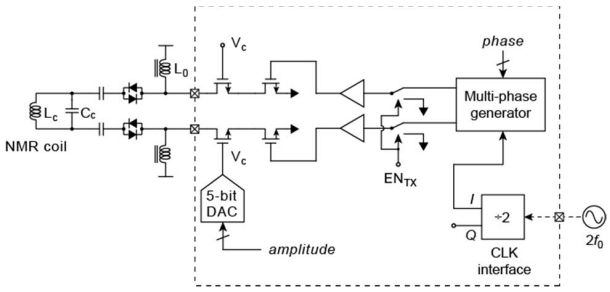

Figure 4. Architecture of the RF transmitter.

Figure 3 describes the operation of the APS, which consists of three blocks: a pulse memory, a pulse counter, and a pulse programmer. An arbitrary NMR pulse sequence is stored in the memory in the form of 64 pulse codes. Each pulse code is 64-bit wide and represents two phases: a TX phase and an RX phase. During the TX phase, the TX transmits an RF pulse with given *amplitude*, *width*, and *phase* (the RX can be also turned on at the same time as the TX, for instance, to sense the resonance of the NMR coil; see Fig. 7). And for the RX phase, the TX is turned off during a given time duration, *pulse spacing*, while the RX can be turned on for signal detection (Fig. 3, top center). The pulse programmer is the block that executes these pulse codes by turning on and off the TX and the RX, driving the DAC, and controlling the MPG. (Fig. 3, bottom left). The pulse counter is the block that points to the memory address of the pulse code to run. It increments the memory address after the execution of each pulse code unless a loop is defined. A loop can be defined in a pulse sequence when the loop's start and end are defined in the pulse codes. When the pulse counter reaches the end address of the defined loop, it returns back to the start address of the loop. This loop feature is useful when repetitive pulse sequences are used (*e.g.*, Carr-Purcell-Meiboom-Gill pulse sequence). Users can update the pulse codes in the memory via Serial Peripheral Interface (SPI).

Figure 3, right shows an example of six different RF pulse sequences produced by the IC, which are part of the pulse sequences used for *J*-resolved 2D NMR spectroscopy. Each sequence consists of three pulse codes: one that defines π/2-duration pulse (0° phase) and a time duration Δt (RX off), one that defines a π-duration pulse (180° phase) and a time duration Δt plus a π/2 duration (RX off), and one that defines RX acquisition (RX on). Here π/2-duration is 3 μs. The six sequences use different Δt values with an increment of 6 μs, corresponding to six different sets of codes refreshed in the memory.

Figure 4 shows the architecture of the TX configured in class-E topology. When the TX is turned on by the APS, the switching power amplifier (PA) drives the NMR coil resonantly tuned at the Larmor frequency f_0 (*e.g.*, f_0 = 21.84 MHz in a 0.51-T magnetic field for ^{1}H nuclear spins) with a f_0 clock whose phase is chosen from the MPG's 32 phase outputs. The amplitude control for an RF pulse is achieved by the impedance control of the cascode transistors in the PA whose gate voltages, V_c, can be adjusted by a 5-bit DAC

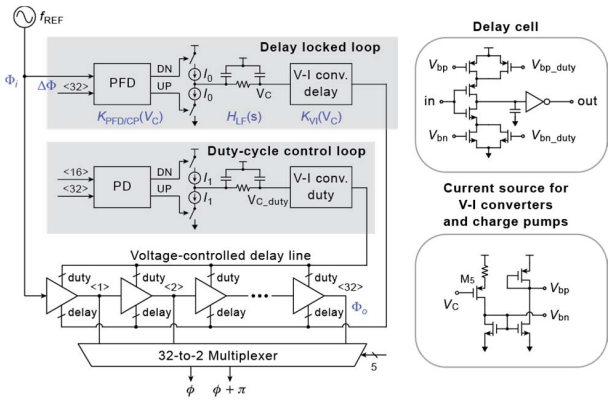

Figure 5. Multiphase generator and its sub circuits.

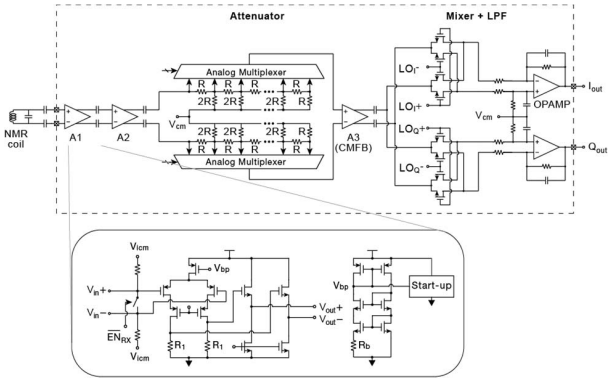

Figure 6. Architecture of the RF receiver.

according to the APS. The DAC uses resistor-string DAC topology with a combination of a 8-resistor string and a 4-resistor string. External anti-parallel diodes are used to isolate the NMR coil from the PA when the TX is off.

Figure 5 shows the MPG and its subcircuits that provides one of the 32 phased clock signals for the PA. Multiple clock phases are necessary in multi-dimensional pulsed NMR spectroscopy to manipulate NMR spins and their interactions in a broad variety of ways. The MPG uses delay-locked loop (DLL) topology to generate the 32 different phases from a single-phase clock input. The DLL uses a phase-frequency detector, a charge pump, a loop filter, a voltage-to-current converter, and a voltage-controlled delay line (VCDL). The DLL is made to support a wide range of Larmor frequencies, as they vary considerably, depending on the types of NMR active nuclei and the strength of the static magnetic field. To support this wide frequency range, the loop bandwidth of the DLL is made to change with respect to its reference input frequency (f_{REF}). For example, the charge pump current is reduced for lower frequency input, which leads to lower loop gain and thus lower loop bandwidth. Expeirmentally, the MPG is verified to work from 1 MHz to 90 MHz. Meanwhile, the MPG also uses a duty-cycle control loop, because duty cycle fluctuation can cause distortion in the PA's output. The duty-cycle loop uses PD to detect overlappings of 16th output

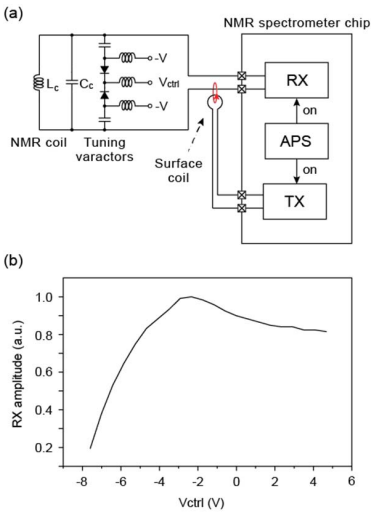

Figure 7. Example of NMR coil tuning. (a) The circuit configuration with a small surface coil for injecting RF into the tank circuit for circuit tuning. (b) Received signal as a function of V_{ctrl}. Maximum signal is reached when V_{ctrl} = -2.335 V, corresponding to the circuit resonance.

and 32nd output, each of them respectfully corresponding to π and 2π in phase.

Figure 6 shows the RX architecture and its sub-circuits. The gain stages use differential common source topology with resistive load, achieving an input-referred noise of 0.82 nV/√Hz at f_0 = 21.84 MHz. The NMR coil is resonantly tuned with a parallel capacitor at f_0 for noise matching. The measured NF is only 0.23 dB. In addition, the gain stages are biased in a way that their gains g_mR_1 are temperature insensitive; the bias circuit (Fig. 6, bottom right) creates a bias current that keeps the gain stage's g_m proportional to $1/R_B$, making the gain proportional to R_1/R_B, which remains temperature insensitive because R_1 and R_B have the same temperature coefficient. To increase the dynamic range, the gain of the entire RX is controlled by the differential R-2R attenuator, which has 12 attenuation levels with a step of 6 dB (0 ~ -66 dB). The amplified signal is then down-converted to the audio frequency using passive quadrature mixers, and the resulting in-phase (I) and quadrature (Q) signals are low-pass filtered by Op-amp based low pass filter (LPF). The overall RX signal path is also temperature insensitive as we use the digitally-controlled attenuator and the passive mixers.

III. Experimental Results

Figure 7 shows an example where the TX and the RX are both turned on by the APS to adjust the resonance frequency of the NMR coil tank circuit to the target frequency f_0. In Fig. 7(a), a small surface coil driven by the TX at the frequency f_0 injects a small fraction of an RF power into the NMR coil tank circuit, whose resonance frequency is controlled by a back-to-back varactor network. When the NMR coil tank circuit is at resonance, a maximum voltage is reached at the RX, with bias voltage V_{ctrl} of -2.3 V in Fig. 7(b).

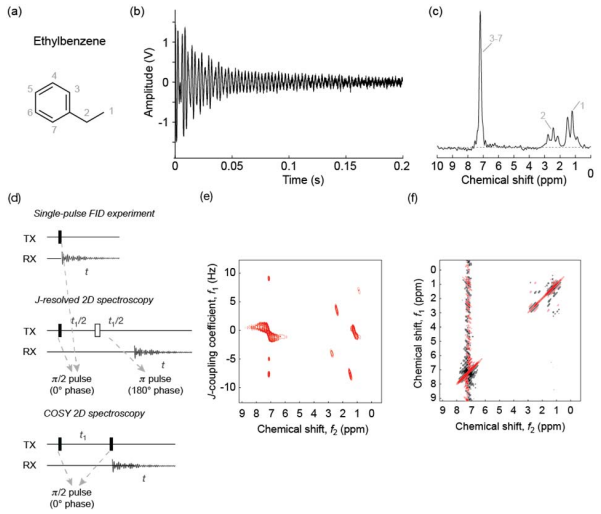

Figure 8. Measured 1D and 2D NMR spectra of ethylbenzene.

Figure 8 shows example NMR spectroscopy data of ethylbenzene ($C_6H_5CH_2CH_3$), obtained by using our NMR spectrometer IC in conjunction with the 0.51-T NdFeB Halbach magnet (Fig. 1; Larmor frequency: 21.84 MHz). A capillary tube is used to transport the sample to the homogeneous volume, around which the NMR coil (173 nH, Q = 31.5) is wound. After running a single pulse free-induction decay (FID) experiment, time domain waveforms from RX's in-phase output is plotted in Fig. 8(b). Fourier transform of the complex signal (I+jQ) yields 1D spectrum of Fig. 8(c) (only real part is shown). The measured spectra are often blurry due to magnetic field drifts caused by temperature fluctuations; those spectra can be recovered by the 1D frequency fluctuation calibration technique presented in [1]. The peaks assigned with the number 1, 2, and 3-7 correspond to ^{1}H spins in the CH_3, CH_2, and C_6H_5 groups, respectively. Multiple peaks in the peak 1 and 2 are due to J-coupling between the CH_3 and CH_2 groups. Figure 8(e) shows the acquired spectrum from the J-resolved 2D spectroscopy pulse sequence (Fig. 8(d), middle). This pulse sequence is intended to investigate coupling coefficients of each peak group; vertical separations of ~7 ppm at the chemical shift f_2 ~ 1 ppm and 2 ppm indicate the existence of the three-bond J-couplings in those spins (noisy peaks at f_2 ~ 7 ppm is called t_1 noise due to large peak magnitude of the peak 3-7). The method to obtain 2D spectrum is as follows: many waveforms with increasing t_1 values are obtained; each waveform is Fourier-transformed; then, those spectra are Fourier-transformed with respect to t_1 values (increment of 20 ms up to 400 ms). Figure 8(f) shows the acquired spectrum from the 2D correlation spectroscopy (COSY) pulse sequence. The pulse sequence is intended to determine couplings between different peak groups; off-diagonal peaks at $\{f_1, f_2\}$ ~ {1.2 ppm, 2.5 ppm}, $\{f_1, f_2\}$ ~ {2.5 ppm, 1.2 ppm} unambiguously reveal the inter-atomic coupling between the CH_3 and CH_2 groups. Both 2D spectra in Figs. 8(e-f) are recovered by the 2D frequency fluctuation calibration technique presented in [1].

IV. Conclusion

We have given a review of the design of our NMR spectrometer IC [1], where its high degree of integration enables a broad repertoire of multi-dimensional NMR spectroscopies (more experimental results can be found in Ref. [1]). Combined with small spectroscopy-grade permanent magnets, as demonstrated in [1] with an example shown in this review paper, the spectrometer IC can enable portable NMR spectroscopy for small-molecule applications. The scalability of the spectrometer IC may also enable high-throughput analysis via massive parallelization and phased-array imaging in conjunction with large superconducting magnets (beyond the portable NMR application), providing a useful tool that combines the solid-state integrated circuits technology and the NMR technology that has been one of the most paramount analytical methods in medicine and biology.

References

[1] D. Ha, J. Paulsen, N. Sun, Y.-Q. Song, and D. Ham, "Scalable NMR spectroscopy with semiconductor chips," *Proc. Natl. Acad. Sci. U.S.A.*, vol. 111, no. 33, pp. 11955–11960, Aug. 2014.

[2] A. J. Baldwin and L. E. Kay, "NMR spectroscopy brings invisible protein states into focus.," *Nature Chemical Biology*, vol. 5, no. 11, pp. 808–814, Nov. 2009.

[3] J. K. Nicholson and J. C. Lindon, "Systems biology: Metabonomics.," *Nature*, vol. 455, no. 7216, pp. 1054–1056, Oct. 2008.

[4] M. Pellecchia, D. S. Sem, and K. Wüthrich, "NMR in drug discovery.," *Nat Rev Drug Discov*, vol. 1, no. 3, pp. 211–219, Mar. 2002.

[5] K. Inomata, A. Ohno, H. Tochio, S. Isogai, T. Tenno, I. Nakase, T. Takeuchi, S. Futaki, Y. Ito, H. Hiroaki, and M. Shirakawa, "High-resolution multi-dimensional NMR spectroscopy of proteins in human cells.," *Nature*, vol. 458, no. 7234, pp. 106–109, Mar. 2009.

[6] B. Luy, "Towards portable high-resolution NMR spectroscopy.," *Angew. Chem. Int. Ed. Engl.*, vol. 50, no. 2, pp. 354–356, Jan. 2011.

[7] J. Anders, G. Chiaramonte, P. SanGiorgio, and G. Boero, "A single-chip array of NMR receivers.," *J. Magn. Reson.*, vol. 201, no. 2, pp. 239–249, Dec. 2009.

[8] J. Anders, P. SanGiorgio, and G. Boero, "A fully integrated IQ-receiver for NMR microscopy.," *J. Magn. Reson.*, vol. 209, no. 1, pp. 1–7, Mar. 2011.

[9] J. Kim, B. Hammer, and R. Harjani, "A 5–300MHz CMOS transceiver for multi-nuclear NMR spectroscopy," presented at the Custom Integrated Circuits Conference (CICC), 2012 IEEE, 2012, pp. 1–4.